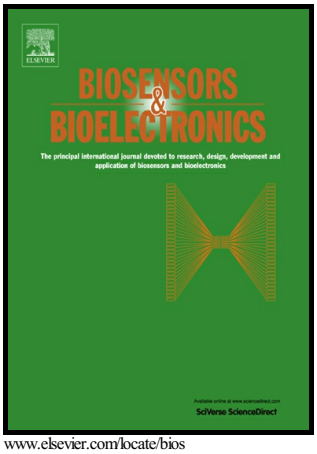

www.elsevier.com/locate/bios

Upconversion nanoparticles based FRET aptasensor for rapid and ultrasenstive bacteria detection

Birui Jin, Shurui Wang, Min Lin, Ying Jin, Shujing Zhang, Xingye Cui, Yan Gong, Ang Li, Feng Xu, Tian Jian Lu

PII: S0956-5663(16)31045-4
DOI: http://dx.doi.org/10.1016/j.bios.2016.10.029
Reference: BIOS9251

To appear in: *Biosensors and Bioelectronic*

Received date: 28 June 2016
Revised date: 24 September 2016
Accepted date: 18 October 2016

Cite this article as: Birui Jin, Shurui Wang, Min Lin, Ying Jin, Shujing Zhang, Xingye Cui, Yan Gong, Ang Li, Feng Xu and Tian Jian Lu, Upconversion nanoparticles based FRET aptasensor for rapid and ultrasenstive bacteria detection, *Biosensors and Bioelectronic* http://dx.doi.org/10.1016/j.bios.2016.10.029

Upconversion nanoparticles based FRET aptasensor for rapid and ultrasenstive bacteria detection

Birui Jin [1,3], Shurui Wang[2,3], Min Lin[2,3*], Ying Jin[4], Shujing Zhang[4], Xingye Cui[2,3], Yan Gong[2,3], Ang Li[6], Feng Xu [2,3], Tian Jian Lu [3,5]

[1] State Key Laboratory for Mechanical Behavior of Materials, Xi'an Jiaotong University, Xi'an 710049, P.R. China

[2] MOE Key Laboratory of Biomedical Information Engineering, Xi'an Jiaotong University, Xi'an 710049, P.R. China

[3] Bioinspired Engineering and Biomechanics Center (BEBC), Xi'an Jiaotong University, Xi'an 710049, P.R. China

[4] Key Laboratory of Space Nutrition and Food Engineering, China Astronauts Research and Training Center, Beijing 100094, P.R. China

[5] MOE Key Laboratory for Multifunctional Materials and Structures, Xi'an Jiaotong University, Xi'an 710049, P.R. China

[6] Key Laboratory of Shaanxi Province for Craniofacial Precision Medicine Research, College of Stomatology, Xi'an Jiaotong University, Xi'an 710049, PR China

[*]Corresponding author. minlin@mail.xjtu.edu.cn

Abstract

Pathogenic bacteria cause serious harm to human health, which calls for the development of advanced detection methods. Herein, we developed a novel detection platform based on fluorescence resonance energy transfer (FRET) for rapid, ultrasensitive and specific bacteria detection, where gold nanoparticles (AuNPs, acceptor) were conjugated with aptamers while upconversion nanoparticles (UCNPs, donor) were functionalized with corresponding complementary DNA (cDNA). The spectral overlap between UCNPs fluorescence emission and AuNPs absorption enables the occurrence of FRET when hybridizing the targeted aptamer and cDNA, causing upconversion fluorescence quenching. In the presence of target bacteria, the aptamers preferentially bind to bacteria forming a three-dimensional structure and thereby dissociate UCNPs-cDNA from AuNPs-aptamers, resulting in the recovery of

upconversion fluorescence. Using the UCNPs based FRET aptasensor, we successfully detected *E. coli* ATCC 8739 (as a model analyte) with a detection range of 5-10^6 cfu/mL and detection limit of 3 cfu/mL. The aptasensor was further used to detect *E.coli* in real food and water samples (*e.g.*, tap/pond water, milk) within 20 minutes. The novel UCNPs based FRET aptasensor could be used to detect a broad range of targets from whole cells to metal ions by using different aptamer sequences, holding great potential in environmental monitoring, medical diagnostics and food safety analysis.

Keywords

Upconversion nanoparticle; Gold nanoparticle; Aptamer; E.coli ATCC 8739; Microorganism detection

1 Introduction

Bacteria are closely related to human health: pathogenic bacteria can cause a variety of diseases via food and water even at a very low concentration (Zuo et al. 2013). According to the statistical data from the World Health Organization in 2015, 600 million people (almost 1 in 10) in the world suffered from diseases caused by pathogenic bacteria-contaminated food, among which 420,000 people dead (Chaib 2015). Thus, technologies capable of rapid and ultrasensitive detection of pathogenic bacteria are of great importance for food and water safety. Existing strategies for bacteria detection are mainly based on colony culture and counting (Tsougeni et al. 2016), polymerase chain reaction (PCR) (Morales-Narvaez et al. 2015), and enzyme-linked immune-sorbent assay (ELISA) (Wu et al. 2015b). However, several limitations are associated with these methods, such as long detection time and complicated operation (Abbaspour et al. 2015; Lian et al. 2014; Yoo et al. 2015), which limit their widespread applications. Therefore, novel approaches are needed for rapid and ultrasensitive bacteria detection.

Lanthanide-doped upconversion nanoparticles (UCNPs) are capable of emitting visible luminescence under near infrared (NIR) excitation (Shao et al. 2014), which offer excellent photo-stability, narrow emission spectrum, less toxic elements multicolor tunable property and low background fluorescence, *etc.* (Feng et al. 2015b; Lin et al. 2014a; Wang and Liu 2014). UCNPs thus hold great promise for bio-detection based on fluorescence labeling (Han et al. 2014; Li et al. 2012; Lin et al. 2012; Shao et al. 2014). Actually, UCNPs have been used for bacteria detection based on antibody and antigen recognition (Morales-Narvaez et al. 2015; Niedbala et al. 2001; Ong et al. 2014; Wu et al. 2014c). However, antibodies are redox sensitive and vulnerable to changes in environmental (solution) pH and temperature, leading to short shelf life and the requirement of low temperature storage (Chen and Yang 2015).

Aptamer is a promising candidate as a potential substitute for antibody, which is a kind of ssDNA or RNA molecules that bind to their targets to form a three-dimensional structure with high affinity and specificity (Deng et al. 2015).

Aptamers have functions similar to antibodies (*e.g.*, targeted binding) but exhibit a variety of advantages, such as selective binding to various targets (from ions to whole cells), easy synthesis by chemical routes, good stability to changes in pH and temperature (Wu et al. 2014b). In addition, aptamers can be easily modified with a variety of tags (*e.g.*, gold nanoparticles, fluorescence materials), providing extraordinary flexibility in the development of assays (Chen and Yang 2015). Pioneering works using aptamer and nanoparticles for sensing have been intensively studied, such as aptamers have been used to detect bacteria (Ozalp et al. 2015), enzyme (Zheng et al. 2012), protein (Wei et al. 2015), whole cell (Wang et al. 2015) and ions (Chung et al. 2013). Excellent reviews on this topic could be found in literatures (Dong et al. 2014; Han et al. 2010; Iliuk et al. 2011). Actually, with the assistance of magnetic beads for target separation, aptamers conjugated UCNPs have been employed to detect several pathogenic bacteria (Duan et al. 2012; Wu et al. 2014b). However, the presence of magnetic beads (Fe_3O_4) deepens the color of the solution and affects the fluorescence intensity of the final probe complex, yielding a reduced detection limit (Duan et al. 2012). Further, although the concentration effect of magnetic beads was avoided via subtraction of background signal by re-designing the detection probe (Wu et al. 2014b), this method still suffers from the potential loss of sample during magnetically assisted separation and washing steps. Fluorescence resonance energy transfer (FRET) based technology has been widely applied in ultrasensitive detection, which requires no sample separation and washing steps (Zhang et al. 2015). FRET is a process that employs fluorescence particles as donors and quencher particles as acceptors, where the fluorescence of the donor can be quenched by the acceptor when the donor is immediately adjacent (< 10 nm) the acceptor (Liu et al. 2013). The change of fluorescence intensity before and after quenching may be used to monitor the concentrations of targets. Although the integration of UCNPs and aptamer or oligonucleotides using FRET technology have been developed for DNA, ions and small molecules detection (Liu et al. 2013; Ma et al. 2014; Wu et al. 2014a; Wu et al. 2015a), these FRET systems have not yet been explored for bacteria detection.

Herein, we developed a rapid, ultrasensitive and specific FRET based bacteria detection method. Gold nanoparticles (AuNPs) were conjugated with bacteria targeting aptamers (serving as fluorescence acceptors), while UCNPs functionalized with another aptamer complementary DNA sequence were employed as fluorescence donors. Via complementary pairing of cDNA and aptamers, the FRET occurred due to spectral overlap, leading to fluorescence quenching between the AuNPs and the UCNPs. In the presence of target bacteria, the aptamers preferentially bound to the target bacteria and caused aptamers dissociation from cDNA, thereby liberating UCNPs and resulting in fluorescence recovery. This novel detection system avoids target separation procedures and enables rapid, ultrasensitive and specific bacteria detection. The developed method paves the way for rapid, ultrasensitive and specific detection of pathogenic bacteria, heavy metal and viruses for food and water safety.

2 Materials and methods

2.1 Materials

$YCl_3 \cdot 6H_2O$, $ErCl_3 \cdot 6H_2O$, $YbCl_3 \cdot 6H_2O$, $GdCl_3 \cdot 6H_2O$, NH_4F, 1-Ethyl-3-(3-dimethylaminopropyl)-carbodiimide hydrochloride (EDC), N-hydroxysulfosuccinimide sodium salt (sulfo-NHS) and Tris (2-carboxyethyl) phosphine (TCEP) were obtained from Sigma Aldrich. Oleic acid (90%) and 1-Octacene (90%) sodium were purchased from Alfa Aesar. Methanol, NaOH , ethanol, and chloroform were obtained from Tianjin Zhiyuan Chemical Reagent Co., Ltd. Poly(acrylic acid) (PAA, Mw= 800–1000) were obtained from Tianjin Yongsheng Chemical Reagent Co., Ltd. Trisodium citrate and Sodium dodecyl sulfate (SDS) were purchased from LLC (Solon, OH, USA). Chloroauric acid was purchased from Sinopharm Chemical Reagent Co., Ltd. (Shanghai, China). Bacteria aptamers and their complementary strands (**Table 1**) were selected according to literature (Kim et al. 2013) and synthesized by Xi'an Sangon Biological Science & Technology Company. Phosphate buffer saline (PBS, pH= 7.4) was prepared by mixing 0.194 g KCl, 8.010 g

NaCl, 0.191 g KH_2PO_4 and 2.290 g $Na_2HPO_4 \cdot 12H_2O$ in 1 L ultrapure water. All reagents were used without any purification.

2.2 Synthesis and surface modification of $NaYF_4$:Yb/Er UCNPs

Thermal decomposition procedure was applied to synthesize UCNPs, as reported by our previous protocol (Feng et al. 2015a; You et al. 2015). Briefly, $YCl_3 \cdot 6H_2O$ (242.69 mg, 0.8 mmol), $ErCl_3 \cdot 6H_2O$ (7.64 mg, 0.02 mmol) and $YbCl_3 \cdot 6H_2O$ (69.75 mg, 0.18 mmol) were dissolved in ultrapure water (2 mL). The mixture was then added to a flask containing 7.5 mL oleic acid and 15 mL 1-octadecene. The obtained mixture was stirred at room temperature for 0.5 h. The solution was then heated to 120 °C and followed by keeping at 156 °C for 1 h to remove ultrapure water under argon atmosphere protection. The mixture was then cooled down to room temperature. Next, NaOH (100 mg, 2.5 mmol) and 10 mL methanol solution of NH_4F (148.15 mg, 4 mmol) were added into the solution and kept stirring at room temperature for 2 h. After methanol evaporation, the mixture was heated to 280 °C and maintained for 1.5 h before cooling down to room temperature. The product was centrifuged and washed with cyclohexane and ethanol for three times and was finally re-dispersed in 10 mL cyclohexane.

The surface modification was performed by a ligand exchange process. PAA was used as a multidentate ligand to displaces the original hydrophobic ligands on the UCNPs surface by mixing 1 mL ethanol, 1 mL of UCNPs and 14.5 μL PAA. The mixture was dispersed in chloroform (~15 mg/ mL) and subjected to overnight stirring. The product was then centrifuged at 8,000 rpm for 8 min. After washing for three times using ethanol and water separately, the obtained product were re-dispersed in 5 mL ultrapure water.

2.3 Attachment of cDNA to the UCNPs

1 mL as-prepared PAA@UCNPs was centrifuged at 8,000 rpm and re-suspended in 1 mL MES buffer. 120 μL 2mg/mL EDC and 60 μL 2mg/mL sulfo-NHS were subsequently added into the solution. The reaction continued at 37 °C for 2 h. 500 μL 2 nmol/mL cDNA solution was added into the solution. The mixture was then incubated for overnight. Then the cDNA conjugated UCNPs was centrifuged and washed three times with PBS buffer and then finally re-dispersed in 1 mL PBS butter.

2.4 Synthesis of gold nanoparticles and thiolated aptamers conjugation

AuNPs with a mean diameter of 13±3 nm were prepared according to the previously reported method (Hu et al. 2013; Leoni and Legnani 2001). In short, 1.2 mL of 0.825% chloroauric acid and 4.5 mL of 1% trisodium citrate were successively added to three-neck round-bottom, 100 mL boiled ultrapure water containing flask. Then the color of the solution immediately turned from yellow to purple and finally kept wine-red. The generated product was used to prepare AuNPs and oligonucleotide aptamers conjugate.

The thiolated oligonucleotide aptamers were activated for 1 h by adding 4 μL of 10 mM TCEP, 20 μL of acetate buffer (pH 4.76, 500 mM) and 100 μL of ultrapure water to reach a final concentration of 100 μM. And the activated oligonucleotide aptamers were added into the as-prepared AuNPs solution. Then 2 M NaCl and 1% SDS were separately added to the above solution to obtain a final concentration of 0.01% SDS and 0.16 M NaCl. After centrifugation at 14,000 rpm, the red pellet was collected and re-suspended in 1 mL PBS (Leoni and Legnani 2001).

2.5 Bacteria culture and sample suspension preparation

All bacteria strains used in this research were *E. coli* DH5α, *E. coli* (ATCC 8739), *E. coli* (ATCC 25922), bacillus subtilis (ATCC 6633), and staphylococcus aureusc (ATCC 25923). *E. coli* (ATCC 8739) was selected as target bacteria for the detection, meanwhile *E. coli* (ATCC 25922), *E. coli* DH5α, Staphylococcus aureus (ATCC

25923), and bacillus (ATCC 6633) were selected as control groups for detection. All above strains were firstly streaked onto Luria–Bertani (LB) agar plates, and then incubated at 37 °C for 16 h. An isolated colony of each strain was picked and inoculated in 8 mL of LB medium. After incubation at 37 °C for 16 h (shaking at 250 rpm), the bacteria culture was then aliquoted, and applied as a standard stock for all experiments. The *E. coli* stock was firstly diluted by ten-fold using PBS and was then spread on LB agar plates. To fix the original concentration of the *E. coli* stock, single colonies of each bacteria strain were counted after overnight incubation.

2.6 Detection of target bacteria

The as-prepared UCNPs-cDNA were ten times diluted. Then 200 μL of UCNPs-cDNA was hybridized with the optimized AuNPs-aptamers at 37 °C for 10 min to obtain UCNPs-AuNPs FRET aptasensor pairs. The as-prepared aptasensor pair solution was scanned by fluorescence spectrum. 1 to 10^6 cfu/mL of standard target bacteria were subsequently added to the mixture, which was further incubated at 37 °C for 10 min. The upconversion fluorescence intensity of the final mixture were then measured using fluorescence spectrum with an external 980 nm laser as the excitation source in place of the xenon lamp in the spectrometer.

3. Results and Discussion

3.1 Bacteria detection based on FRET between UCNPs and AuNPs

The principle for detecting target bacteria using the FRET pair of UCNPs and AuNPs was schematically described in **Figure 1**. The amino-modified complementary DNA (sequence shown in **Table 1**) aptamers were attached to the carboxyl-functionalized UCNPs by condensation reaction **(Fig. 1A)**. The thiol-modified E.coli ATCC 8739 aptamers capable of target recognition were conjugated to the surface of AuNPs through Au-S chemistry **(Fig. 1B)**. The FRET aptasensor was established between a donor-acceptor pair: UCNPs-cDNA hybridized with AuNPs-aptamers **(Fig. 1C)**. In the absence of *E. coli* ATCC 8739, the 3’ terminals of the aptamers could perfectly complement the cDNA. Thus, the acceptors (AuNPs) and donors (UCNPs) are placed

in close proximity, which results in the quench of green upconverison fluorescence from UCNPs due to their highly overlapped spectrum. By introducing *E. coli* ATCC 8739 into the FRET system, aptamers preferentially bind to target bacteria to form a 3D stem–loop structure and cause the dissociation of aptamers from cDNA, so that aptamers-DNA pairs are destroyed and the green fluorescence recovers (Wu et al. 2014a). The recovery of the upconverison fluorescence intensity is proportional to the target bacteria concentration **(Fig. 1D)**.

3.2 Characterization of UCNPs and AuNPs

To access the morphology, size and surface modification of UCNPs and AuNPs, we conducted a series of characterization. $NaYF_4$ is chosen as host material for upconversion nanoparticles, since fluorides usually exhibit low phonon energies (~350 cm^{-1}) and high chemical stability (Wang and Liu 2009). In addition to host material, the energy difference between each excited level and its lower-lying intermediate level (ground level) should be close enough to facilitate photon absorption and energy transfer steps involved in upconversion processes. Er^{3+} typically features such ladder-like energy levels and is thus frequently used as activator (Wang and Liu 2009). To enhance upconversion fluorescence efficiency, a sensitizer with a sufficient absorption cross-section in the NIR region is usually co-doped along with the activator to take advantage of the efficient energy transfer upconversion process between the sensitizer and activator. Yb^{3+} is particularly suitable as the upconversion sensitizer. The optimized Er^{3+} and Yb^{3+} concentrations have been reported to be 2% and 18% for enhanced upconversion fluorescence efficiency (Lin et al. 2014). XRD patterns indicate that $NaYF_4$: Yb, Er exhibits a pure hexagonal phase, where all of the diffraction peaks can be ascribed to the hexagonal structure of $NaYF_4$ (JCPDS no.16-0334), **Figure S1**. According to existing report, hexagonal-phase $NaYF_4$:Yb/Er materials exhibit about an order of magnitude enhancement of upconversion efficiency as compared to their cubic phase counterparts (Wang and Liu 2009). The representative TEM image of the synthesized UCNPs indicates that the UCNPs are monodispersed with an average diameter of 35

nm (**Fig. 2A**), the molarity of UCNPs was 50 nM (The calculated method was shown in Supplemental Material). PAA modification was realized by ligand exchange to replace the original hydrophobic ligands on the UCNPs surface (Birui et al. 2015). The presence of PAA on the surface of the UCNPs after the ligand exchange could be confirmed by FT-IR spectroscopy (**Fig. S2**). The obtained UCNPs-PAA could be re-dispersed in ultrapure water to exhibit green emission under 980 nm excitation (inset of **Fig. 2A**). The TEM image of UCNPs-PAA shows no obvious aggregation (**Fig. 2B**). We observed a clear polymer layer, ~ 1 nm thick, on the surface of UCNPs from the HRTEM image (inset of **Fig. 2B**). The size distribution of UCNPs-PAA was shown in Figure 2C. PAA-modified UCNPs are negatively charged with Zeta potential of ~-43 mV (Fig. S3). To demonstrate the successful conjugation of cDNA, we measured the absorbance of UCNPs-PAA and UCNPs-cDNA separately. We observed no absorption peak in the UV-vis spectrum of UCNPs-PAA before conjugating with cDNA, while absorption peak at approximately 260 nm was observed in the UV-vis spectrum of UCNPs-PAA after cDNA conjugation through EDC and sulfo-NHS activation (**Fig. 2D**). These results indicate that the UCNPs-PAA have been successfully functionalized with amino-cDNA according to literature (Lin et al. 2011). To further prove that the DNA molecules are conjugated but not absorbed on UCNPs, we performed cDNA and UCNPs reaction without adding EDC and sulfo-NHS. We performed UV-vis absorption spectroscopy of UCNPs solution after reaction (**blue line of Fig. 2D**) and observed no absorption peak at 260 nm in the UV-vis spectrum. The DNA loading density was estimated ~160 per UCNP (calculation method was shown in the Supplemental Materials). We also analyzed the sizes of UCNPs, UCNPs-PAA, UCNPs-PAA-cDNA by DLS and found that UCNPs-PAA, UCNPs-PAA-cDNA were uniformly modified and well dispersed in aqueous solution (**Fig. 2E**). It should be noticed that the DLS results represent the hydrodynamic size of UCNPs (core plus ligands), which is larger than that measured from TEM image (Duan et al. 2013). To describe the stability of DNA-modified UCNPs, we monitored the fluorescence intensity of UCNPs-cDNA (1 nM) in 1 mL PBS for 24 days. The fluorescence intensity as a function of time was shown in Figure

S5A. The fluorescence intensity shows negligible decline over time, indicating that the DNA-modified UCNPs would not aggregated for least 24 days. To further clarify the stability of DNA modified UCNPs, the UCNPs-cDNA (24 days after modification) were used to hybridized with AuNP-aptamers as shown in Figure S5B. The quench values were shown in Figure S5C. We found that the quenching values were also negligible decline over time, indicating that the DNA on the surface of UCNPs had a good stability for least 24 days.

To characterize the prepared AuNPs and AuNPs-aptamers conjugates, we performed TEM and UV/Vis spectrum testing. The TEM image indicates that the prepared AuNPs were mono-dispersed with a diameter of ~13 nm (**Fig. 2F**), the molarity of AuNPs were 4.3 nM. We also tested the Zeta potential of AuNPs which are negatively charged with Zeta potential of ~-40 mV (Fig. S3). AuNPs dispersed in ultrapure water show visible red color (inset of **Fig. 2E**). The size distribution of AuNPs was shown in Figure 2G. It should be noted that UCNPs and AuNPs with similar size dispersion have also been applied in the quantitatively detection of ions or DNA (Duan et al. 2012; Pons et al. 2007), thus will not affect quantitative performance. The UV-vis spectra of both AuNPs and AuNP-aptamers are shown in **Figure. 2H.** A specific absorption peak of AuNPs-aptamers sample at approximately 260 nm could be observed, confirming the presence of aptamers on the surface of AuNPs (Lin et al. 2011). It should be noted that the absorption peak of AuNPs sample experiences a slight red shift from 520 nm to 526 nm (inset of **Fig. 2H**). This shift in the absorbance of AuNPs should be attributed to the functionalization by thiolated DNA (aptamers) (Hu et al. 2013). The DNA loading density was estimated ~21 per AuNP (calculation method was shown in the Supplemental Materials).

3.3 Preparation of UCNPs-AuNPs FRET aptasensor

AuNPs are featured of good absorption property in the visible light region. The AuNPs used in this study exhibit a strong absorption peak at approximately 526 nm (**Fig. 3A** dashed line). This absorption band overlaps with green emission from

UCNPs-PAA that peaks at 540 nm (**Fig. 3A** solid line), suggesting that FRET could take place between the UCNPs-cDNA (donors) and the AuNPs-aptamers (acceptors). To demonstrate the formation of the FERT pair, we added 200 μL UCNPs-cDNA (1 nM) into 1 mL ultrapure water; 40 μL AuNPs-aptamers (4.3 nM) were then repeatedly added, followed by incubation as well as fluorescence spectrum scanning. We found that the upconversion fluorescence of UCNPs-cDNA was gradually quenched as the amount of AuNPs- aptamers was increased (**Fig. 3B**). It should be noted that both the UCNPs-PAA and AuNPs are negatively charged prohibiting absorption between the two particles, suggesting that the formation of FRET pair is based on DNA hybridization. To estimate the FRET efficiency between UCNPs and AuNPs, we calculated the FRET efficiency according to the literature (Pons et al. 2007). Detailed calculation processes could be found in the Supplemental Materials. The dipole orientation factor is κ^2 which equals to 0.67 (Mattsson et al. 2015). The spectral overlap integral $J = 1.39 \times 10^8$ ($M^{-1}cm^{-1}$) which was calculated according to equation (5) in Supplemental Materials. The Förster distance was estimated to be R_0(min) = 7.78 nm or R_0(max) = 11.4 nm considering that Φ (quantum yield of UCNPs) falls between 0.001 and 0.01 (Mattsson et al. 2015). The calculated Förster distance in our study seems to be higher than typical FRET distance (5-10 nm). This is because that the surface plasmon resonances around AuNPs can extend the energy transfer rate and the utility of sensors to a distance of ~20 nm, far beyond the range allowed by "classic" dye-to-dye FRET pairs (Ray et al. 2006). The FRET efficiency was calculated to be η(min) = 55% or η(max)= 92% using the different estimated values of Φ (0.001 and 0.01).

3.4 Optimization of dosages of complementary UCNPs-cDNA and AuNPs-aptamers

AuNPs-aptamers concentration can affect the detection limit. For instance, low AuNPs-aptamers concentration will lead to the formation of low FRET aptasensor concentration, reducing thence the maximum detection limit. Whereas, when

AuNPs-aptamers are in relative excess, the free AuNPs-aptamers can bind to the target bacteria without altering the fluorescence intensity. To optimize the dosages of complementary UCNPs-cDNA and AuNPs-aptamers, we repeatedly added 40 μL (4.3 nM) AuNPs-aptamers into UCNPs-cDNA (200 μL (1 nM) UCNPs-cDNA into 1 mL ultrapure water) for fluorescence intensity analysis with fixed UCNPs-cDNA concentration. We analyzed fluorescence reduction with increasing amount of AuNPs-aptamers (**Fig. S6**), where F and F_0 represent the fluorescence intensity of UCNPs-cDNA before and after adding AuNPs-aptamers, respectively. With increasing AuNPs-aptamers, the formation of FRET pair via UCNPs-cDNA and AuNPs-aptamers hybridization increased, resulting in fluorescence quenching. The optimized dosages of UCNPs-cDNA and AuNPs-aptamers can be fixed when fluorescence quenching reaches equilibrium. Consequently, in subsequent experiments, we fixed the quantity of AuNPs-aptamers at 240 μL and the quantity of UCNPs-cDNA at 200 μL.

3.5 Specificity evaluation

To test the selective targeting capability of FRET aptasensor for *E. coli* ATCC 8739, we added other bacteria (*e.g.*, S.aureus and bacillus) and different E.coli strains (*e.g.*, *E. coli* ATCC 25922 and *E. coli* DH5α) into the sample, **Figure 4**. We observed that only *E. coli* ATCC 8739 (the targeting *E. coli*) induced a dramatic fluorescence recovery at the corresponding upconversion emission peaks (**Fig. 4A**). We further quantified fluorescence intensity recovery for different bacteria and found that S.aureus and bacillus in this system had negligible effect on fluorescence intensity recovery **(Fig. 4B**), which demonstrated that the aptasensor exhibited good specificity from different bacteria types. The specificity of the aptasensor was further confirmed by the significant difference between different strains of *E. coli*, although both *E. coli* ATCC 25922 and *E. coli* DH5α exhibited fluorescence recovery (**Fig. 4B**). This is because that the possible binding targets of aptamers on E.coli surface (e.g., the components of outer cellular membrane of E.coli, outer membrane proteins, and flagella) have similar structures and these targets can be identified via

aptamer-facilitated biomarker discovery during the SELEX process (Kim et al. 2013). Overall, the present result further demonstrates the excellent specificity of the FRET aptasensor.

We added a control experiment using UCNPs (without cDNA conjugation) as donor and AuNPs (or AuNPs-aptamers) as acceptor. The results show that upconversion emission from UCNPs (without cDNA conjugation) could be hardly quenched by either AuNPs (**Fig. S7A**) or AuNPs-aptamers (**Fig. S7B**), suggesting that the FRET probe could not be formed without hybridization between cDNA and aptamers. The results further confirm that the formation of FRET pair is due to the DNA hybridization. Considering that the selected aptamers are specific to *E.coli* ATCC 8739, adding increasing amount of *E.coli* ATCC 8739 results in increased fluorescence intensity (**Fig. 4**), which suggests that the dehybridization of AuNPs from UCNP surface is the result of increased affinity to the bacteria especially for *E.coli* 8739.

3.6 Determination of target bacteria

To evaluate the detection limit of the developed FRET system for target bacteria (*E. coli* ATCC 8739 here), we plotted in **Figure 5A** the calibration curve of the detection system by adding different bacteria concentrations and monitoring the change in fluorescence intensity at 540 nm. We observed that the upconversion fluorescence intensity gradually increases with increasing bacteria concentration and that the E.coli ATCC 8739 concentration is proportional to the increase in upconversion fluorescence intensity (ΔF), with a linear relationship in the detection range of 5-10^6 cfu/mL (**Fig. 5B**). The TEM image of DNA-mediated assembly of AuNPs on UCNP was shown in Figure S8A. A large amount of AuNPs were observed, indicating that AuNPs were successfully combined with UCNPs since centrifugation under 8,000 rpm could not separate free AuNPs from solution. After adding target bacteria, AuNPs-aptamers were dehybridized from UCNPs surface due to the increased affinity between AuNPs-aptamers and target bacteria. The solution was then centrifuged under 3000 rpm to separate AuNPs-aptamers and target bacteria complex. The particles

suspended in the supernate were then observed under TEM and we observed negligible amount of AuNPs (Fig. S8B), suggesting that AuNPs were separated from UCNPs by bacteria. Fluorescence recovery value gradually reached the fluorescence intensity before quenching. It has been commonly accepted that the detection limit equals to three times of detection noise (S/N=3) (Chen et al. 2015; Fang et al. 2015; Mishra et al. 2015). The estimated detection limit is 3 cfu/mL. With the developed aptasensor, the ultrasensitive detection for bacteria can be completed within 20 min without any need for enrichment, which is significantly faster than traditional methods such as colony culture and counting (Tsougeni et al. 2016), PCR (Morales-Narvaez et al. 2015), ELISA (Shih et al. 2015), and the electrode method (Lian et al. 2014). In addition, the sensitivity of the developed aptasensor is comparable or even higher than that achieved in previous studies (Demirkol and Timur 2015; Shangguan et al. 2015), highlighting its potential use for sensitive target detection in the near future.

3.7 Analytical application

The practical application and accuracy of the developed bio-analysis method was evaluated using real samples, including tap/pond water and milk (**Fig. 6**). The real samples were firstly high temperature sterilized. After simple pretreatment (see details presented in supporting information), the samples were spiked with *E. coli* ATCC 8739 with concentrations ranging between 1 and 1×10^4 cfu/mL. It should be noticed that due to the different background of milk and water, we established another calibration curve for the milk sample (**Fig. S9**). The whole detection process was completed in less than 20 min. For either tap/pond water or milk samples, the detected bacteria concentrations by the proposed FRET method were similar to those of the plate-counting method, and no significant difference was observed between the two methods. The application performance clearly demonstrates that the present method based on UCNPs labeling and aptamer targeting can efficiently detect and quantify target bacteria in real samples.

4. Conclusion

We developed an aptasensor via FRET between UCNPs and AuNPs for rapid, ultrasensitive and specific detection of bacteria (*e.g.*, *E. coli* ATCC 8739). The application of near-infrared 980 nm laser excitation for the generation of fluorescence signal avoids possible auto-fluorescence due to biomolecules contained in complex real food and water samples. The use of the FRET system provides an efficient method for E.coli detection in one single step. In addition, unlike traditional antibody-based targeting methods that are temperature sensitive and undergo irreversible antibody denaturation, the aptamer-based targeting method is stable with maintained high specificity to target bacteria. Therefore, aptamer-based targeting offers a novel approach to construct convenient, ultrasensitive, specific, and stable platforms for bio-assays, holding great potential for pathogenic bacteria detection in food and water samples.

Acknowledgements

This research was financially supported by the National Natural Science Foundation of China (11402192), the Fundamental Research Funds for the Central Universities (2016qngz03), and the Open Funding Project of Key Laboratory of Space Nutrition and Food Engineering Laboratory (SNFE-KF-15-09).

References

Abbaspour, A., Norouz-Sarvestani, F., Noori, A., Soltani, N., 2015. Aptamer-conjugated silver nanoparticles for electrochemical dual-aptamer-based sandwich detection of staphylococcus aureus. Biosensors & bioelectronics 68, 149-155.

Birui, J., Min, L., Minli, Y., Yujin, Z., Mingxi, W., Feng, X., Zhenfeng, D., Tianjian, L., 2015. Microbubble embedded with upconversion nanoparticles as a bimodal contrast agent for fluorescence and ultrasound imaging. Nanotechnology 26(34), 345601.

Chaib, F., 2015. WHO's first ever global estimates of foodborne diseases find children under 5 account for almost one third of deaths.

Chen, A., Yang, S., 2015. Replacing antibodies with aptamers in lateral flow immunoassay. Biosensors & bioelectronics 71, 230-242.

Chen, X., Bai, X., Li, H., Zhang, B., 2015. Aptamer-based microcantilever array biosensor for detection of fumonisin B-1. RSC Advances 5(45), 35448-35452.

Chung, C.H., Kim, J.H., Jung, J., Chung, B.H., 2013. Nuclease-resistant DNA aptamer on gold

nanoparticles for the simultaneous detection of Pb2+ and Hg2+ in human serum. Biosensors & bioelectronics 41, 827-832.

Demirkol, D.O., Timur, S., 2015. A sandwich-type assay based on quantum dot/aptamer bioconjugates for analysis ofE. ColiO157:H7 in microtiter plate format. International Journal of Polymeric Materials and Polymeric Biomaterials 65(2), 85-90.

Deng, K., Hou, Z., Li, X., Li, C., Zhang, Y., Deng, X., Cheng, Z., Lin, J., 2015. Aptamer-Mediated Up-conversion Core/MOF Shell Nanocomposites for Targeted Drug Delivery and Cell Imaging. Scientific Reports 5, 7851.

Dong, Y., Xu, Y., Yong, W., Chu, X., Wang, D., 2014. Aptamer and its potential applications for food safety. Critical reviews in food science and nutrition 54(12), 1548-1561.

Duan, J., Yu, Y., Shi, H., Tian, L., Guo, C., Huang, P., Zhou, X., Peng, S., Sun, Z., 2013. Toxic effects of silica nanoparticles on zebrafish embryos and larvae. PLoS One 8(9), e74606.

Duan, N., Wu, S., Zhu, C., Ma, X., Wang, Z., Yu, Y., Jiang, Y., 2012. Dual-color upconversion fluorescence and aptamer-functionalized magnetic nanoparticles-based bioassay for the simultaneous detection of Salmonella Typhimurium and Staphylococcus aureus. Analytica chimica acta 723, 1-6.

Fang, C., Wu, S., Duan, N., Dai, S., Wang, Z., 2015. Highly sensitive aptasensor for oxytetracycline based on upconversion and magnetic nanoparticles. Anal. Methods 7(6), 2585-2593.

Feng, A.L., Lin, M., Tian, L., Zhu, H.Y., Guo, H., Singamaneni, S., Duan, Z., Lu, T.J., Xu, F., 2015a. Selective enhancement of red emission from upconversion nanoparticles via surface plasmon-coupled emission. RSC Advances 5(94), 76825-76835.

Feng, A.L., You, M.L., Tian, L., Singamaneni, S., Liu, M., Duan, Z., Lu, T.J., Xu, F., Lin, M., 2015b. Distance-Dependent Plasmon-Enhanced Fluorescence of Upconversion Nanoparticles using Polyelectrolyte Multilayers as Tunable Spacers. Sci. Rep. 5.

Han, J., Zhang, C., Liu, F., Liu, B., Han, M., Zou, W., Yang, L., Zhang, Z., 2014. Upconversion nanoparticles for ratiometric fluorescence detection of nitrite. Analyst 139(12), 3032-3038.

Han, K., Liang, Z., Zhou, N., 2010. Design strategies for aptamer-based biosensors. Sensors 10(5), 4541-4557.

Hu, J., Wang, L., Li, F., Han, Y.L., Lin, M., Lu, T.J., Xu, F., 2013. Oligonucleotide-linked gold nanoparticle aggregates for enhanced sensitivity in lateral flow assays. Lab on a chip 13(22), 4352-4357.

Iliuk, A.B., Hu, L., Tao, W.A., 2011. Aptamer in bioanalytical applications. Anal Chem 83(12), 4440-4452.

Kim, Y.S., Song, M.Y., Jurng, J., Kim, B.C., 2013. Isolation and characterization of DNA aptamers against Escherichia coli using a bacterial cell-systematic evolution of ligands by exponential enrichment approach. Analytical biochemistry 436(1), 22-28.

Leoni, E., Legnani, P.P., 2001. Comparison of selective procedures for isolation and enumeration of Legionella species from hot water system. Journal of Applied Microbiology 90(1), 27-33.

Li, L.L., Zhang, R., Yin, L., Zheng, K., Qin, W., Selvin, P.R., Lu, Y., 2012. Biomimetic surface engineering of lanthanide-doped upconversion nanoparticles as versatile bioprobes. Angewandte Chemie 51(25), 6121-6125.

Lian, Y., He, F., Wang, H., Tong, F., 2014. A new aptamer/graphene interdigitated gold electrode piezoelectric sensor for rapid and specific detection of Staphylococcus aureus. Biosensors & bioelectronics 65C, 314-319.

Lin, M., Zhao, Y., Liu, M., Qiu, M., Dong, Y., Duan, Z., Li, Y.H., Pingguan-Murphy, B., Lu, T.J., Xu, F., 2014a. Synthesis of upconversion NaYF4:Yb3+,Er3+ particles with enhanced luminescent intensity through

control of morphology and phase. Journal of Materials Chemistry C 2(19), 3671.

Lin, M., Zhao, Y., Liu, M., Qiu, M., Dong, Y., Duan, Z., Li, Y.H., Pingguan-Murphy, B., Lu, T.J., Xu, F., 2014b. Synthesis of upconversion NaYF4:Yb3+,Er3+particles with enhanced luminescent intensity through control of morphology and phase. J. Mater. Chem. C 2(19), 3671-3676.

Lin, M., Zhao, Y., Wang, S., Liu, M., Duan, Z., Chen, Y., Li, F., Xu, F., Lu, T., 2012. Recent advances in synthesis and surface modification of lanthanide-doped upconversion nanoparticles for biomedical applications. Biotechnology advances 30(6), 1551-1561.

Lin, Y.-W., Liu, C.-W., Chang, H.-T., 2011. Fluorescence detection of mercury(II) and lead(II) ions using aptamer/reporter conjugates. Talanta 84(2), 324-329.

Liu, J., Cheng, J., Zhang, Y., 2013. Upconversion nanoparticle based LRET system for sensitive detection of MRSA DNA sequence. Biosensors and Bioelectronics 43, 252-256.

Ma, X., Li, S., Xia, Y., Wang, Z., 2014. Determination ofSalmonella typhimuriumby a Fluorescence Resonance Energy Transfer Biosensor Using Upconversion Nanoparticles as Labels. Analytical Letters 47(12), 2048-2060.

Mattsson, L., Wegner, K.D., Hildebrandt, N., Soukka, T., 2015. Upconverting nanoparticle to quantum dot FRET for homogeneous double-nano biosensors. RSC Advances 5(18), 13270-13277.

Mishra, R.K., Hayat, A., Catanante, G., Ocana, C., Marty, J.L., 2015. A label free aptasensor for Ochratoxin A detection in cocoa beans: An application to chocolate industries. Analytica chimica acta 889, 106-112.

Morales-Narvaez, E., Naghdi, T., Zor, E., Merkoci, A., 2015. Photoluminescent Lateral-Flow Immunoassay Revealed by Graphene Oxide: Highly Sensitive Paper-Based Pathogen Detection. Anal Chem 87(16), 8573-8577.

Niedbala, R.S., Feindt, H., Kardos, K., Vail, T., Burton, J., Bielska, B., Li, S., Milunic, D., Bourdelle, P., Vallejo, R., 2001. Detection of analytes by immunoassay using up-converting phosphor technology. Analytical biochemistry 293(1), 22-30.

Ong, L.C., Ang, L.Y., Alonso, S., Zhang, Y., 2014. Bacterial imaging with photostable upconversion fluorescent nanoparticles. Biomaterials 35(9), 2987-2998.

Ozalp, V.C., Bayramoglu, G., Erdem, Z., Arica, M.Y., 2015. Pathogen detection in complex samples by quartz crystal microbalance sensor coupled to aptamer functionalized core-shell type magnetic separation. Analytica chimica acta 853, 533-540.

Pons, T., Medintz, I.L., Sapsford, K.E., Higashiya, S., Grimes, A.F., English, D.S., Mattoussi, H., 2007. On the quenching of semiconductor quantum dot photoluminescence by proximal gold nanoparticles. Nano letters 7(10), 3157-3164.

Ray, P.C., Fortner, A., Darbha, G.K., 2006. Gold nanoparticle based FRET assay for the detection of DNA cleavage. The journal of physical chemistry. B 110(42), 20745-20748.

Shangguan, J., Li, Y., He, D., He, X., Wang, K., Zou, Z., Shi, H., 2015. A combination of positive dielectrophoresis driven on-line enrichment and aptamer-fluorescent silica nanoparticle label for rapid and sensitive detection of Staphylococcus aureus. Analyst 140(13), 4489-4497.

Shao, W., Chen, G., Ohulchanskyy, T.Y., Kuzmin, A., Damasco, J., Qiu, H., Yang, C., Ågren, H., Prasad, P.N., 2014. Lanthanide-Doped Fluoride Core/Multishell Nanoparticles for Broadband Upconversion of Infrared Light. Advanced Optical Materials 3(4), 575-582.

Shih, C.-M., Chang, C.-L., Hsu, M.-Y., Lin, J.-Y., Kuan, C.-M., Wang, H.-K., Huang, C.-T., Chung, M.-C., Huang, K.-C., Hsu, C.-E., Wang, C.-Y., Shen, Y.-C., Cheng, C.-M., 2015. Paper-based ELISA to rapidly detect Escherichia coli. Talanta 145, 2-5.

Tsougeni, K., Papadakis, G., Gianneli, M., Grammoustianou, A., Constantoudis, V., Dupuy, B., Petrou, P., Kakabakos, S., Tserepi, A., Gizeli, E., 2016. Plasma nanotextured polymeric lab-on-a-chip for highly efficient bacteria capture and lysis. Lab on a chip 16(1), 120-131.

Wang, F., Liu, X., 2009. Recent advances in the chemistry of lanthanide-doped upconversion nanocrystals. Chemical Society reviews 38(4), 976-989.

Wang, F., Liu, X., 2014. Multicolor tuning of lanthanide-doped nanoparticles by single wavelength excitation. Accounts of chemical research 47(4), 1378-1385.

Wang, K., Fan, D., Liu, Y., Wang, E., 2015. Highly sensitive and specific colorimetric detection of cancer cells via dual-aptamer target binding strategy. Biosensors & bioelectronics 73, 1-6.

Wei, Y., Zhou, W., Liu, J., Chai, Y., Xiang, Y., Yuan, R., 2015. Label-free and homogeneous aptamer proximity binding assay for fluorescent detection of protein biomarkers in human serum. Talanta 141, 230-234.

Wu, S., Duan, N., Shi, Z., Fang, C., Wang, Z., 2014a. Dual fluorescence resonance energy transfer assay between tunable upconversion nanoparticles and controlled gold nanoparticles for the simultaneous detection of Pb2+ and Hg2+. Talanta 128, 327-336.

Wu, S., Duan, N., Shi, Z., Fang, C., Wang, Z., 2014b. Simultaneous Aptasensor for Multiplex Pathogenic Bacteria Detection Based on Multicolor Upconversion Nanoparticles Labels. Analytical Chemistry 86(6), 3100-3107.

Wu, S., Duan, N., Zhang, H., Wang, Z., 2015a. Simultaneous detection of microcysin-LR and okadaic acid using a dual fluorescence resonance energy transfer aptasensor. Anal Bioanal Chem 407(5), 1303-1312.

Wu, W., Zhao, S., Mao, Y., Fang, Z., Lu, X., Zeng, L., 2015b. A sensitive lateral flow biosensor for Escherichia coli O157:H7 detection based on aptamer mediated strand displacement amplification. Analytica chimica acta 861, 62-68.

Wu, Y.-M., Cen, Y., Huang, L.-J., Yu, R.-Q., Chu, X., 2014c. Upconversion fluorescence resonance energy transfer biosensor for sensitive detection of human immunodeficiency virus antibodies in human serum. Chemical Communications 50(36), 4759-4762.

Yoo, S.M., Kim, D.K., Lee, S.Y., 2015. Aptamer-functionalized localized surface plasmon resonance sensor for the multiplexed detection of different bacterial species. Talanta 132, 112-117.

You, M., Zhong, J., Hong, Y., Duan, Z., Lin, M., Xu, F., 2015. Inkjet printing of upconversion nanoparticles for anti-counterfeit applications. Nanoscale 7(10), 4423-4431.

Zhang, H., Fang, C., Wu, S., Duan, N., Wang, Z., 2015. Upconversion luminescence resonance energy transfer-based aptasensor for the sensitive detection of oxytetracycline. Analytical biochemistry 489, 44-49.

Zheng, D., Zou, R., Lou, X., 2012. Label-free fluorescent detection of ions, proteins, and small molecules using structure-switching aptamers, SYBR Gold, and exonuclease I. Anal Chem 84(8), 3554-3560.

Zuo, P., Li, X., Dominguez, D.C., Ye, B.C., 2013. A PDMS/paper/glass hybrid microfluidic biochip integrated with aptamer-functionalized graphene oxide nano-biosensors for one-step multiplexed pathogen detection. Lab on a chip 13(19), 3921-3928.

Figure 1. Schematic illustration of upconversion nanoparticles based FRET aptasensor for rapid and ultrasenstive bacteria detection. (A) The amino-modified

complementary DNA of the aptamer is attached to the carboxyl-functionalized UCNPs by condensation reaction (B) Conjugating thiol-modified aptamers to the AuNPs through Au-S chemistry. (C) The FRET system is established between a donor-acceptor pair: UCNPs-cDNA hybridized with AuNPs-aptamers. (D) By introducing target bacteria into the FRET system, aptamers preferentially bind to target bacteria resulting in the dissociation of cDNA, thereby aptamers-DNA pairs are destroyed and the green fluorescence recovers.

Figure 2. Characterization of UCNPs and AuNPs. (A) TEM of UCNPs, inset shows photograph of UCNPs excited by a 980 nm laser. (B) TEM of PAA modified UCNPs, inset shows the HRTEM image. (C) The size distribution of UCNPs. (D) The UV-vis absorption spectra of DNA molecules and UCNPs complex. (E) DSL of UCNPs, UCNPs-PAA, UCNPs-PAA-cDNA. (F) TEM of AuNPs, inset shows photograph of AuNPs solution. (G) The size distribution of AuNPs. (H) UV-vis absorption spectra of AuNPs and AuNPs- aptamers. The inset shows the absorption peak of AuNPs sample experiences a slight red shift from 520 nm to 526 nm.

Figure 3. The spectral overlap of AuNPs and UCNPs. (A) UV-vis absorption spectrum of AuNPs (dashed line) and upconversion fluorescence emission spectrum of UCNPs (solid line). (B) The FRET between UCNPs-cDNA and AuNPs-aptamers. The molarity of UCNPs and AuNPs are 1 nM and 4.3 nM in the stock solution, respectively.

Figure 4. Change in upconversion fluorescence with varying types of bacteria. (Concentration of each bacteria was 10^4 cfu/mL.) (A) Fluorescence recovery results of different types of bacteria. (B) Quantification analysis of fluorescence recovery response for different types of bacteria.

Figure 5. Detection of target bacteria with different concentrations. (A) Fluorescence recovery results of target bacteria with different concentrations. (B) Standard curve of relative upconversion fluorescence intensity ($F- F_0$) versus

bacteria concentration.

Figure 6. Relationship between the developed method and the official standard method for E.coli ATCC 8739 detection in (A) tap water, (B) pond water and (C) milk.

Table 1 The sequences of the aptamer and the complementary DNA of the *E. coli* ATCC 8739 aptamer.

Sample Name	Sequence (5′ -3′)
E.coli ATCC 8739 aptamer	GCAATGGTACGGTACTTCCCCATGAGTGTTG TGAAATGTTGGGACACTAGGTGGCATAGAGC CGCAAAAGTGCACGCTACTTTGCTAA-NH_2
Complementary DNA of aptamer	SH-TTAGCAAAGTAGCGTGCACTTTTG

Highlights

A novel UCNPs based FRET aptasensor was first developed to detect bacteria.

This novel detection system avoids target separation procedures and enables rapid, ultrasensitive and specific bacteria detection.

The sensitivity of the developed aptasensor reaches detection limit of 3 cfu/mL, which is comparable or even higher than that achieved in previous studies.

The aptasensor was further used to detect *E.coli* in tap/pond water and milk.

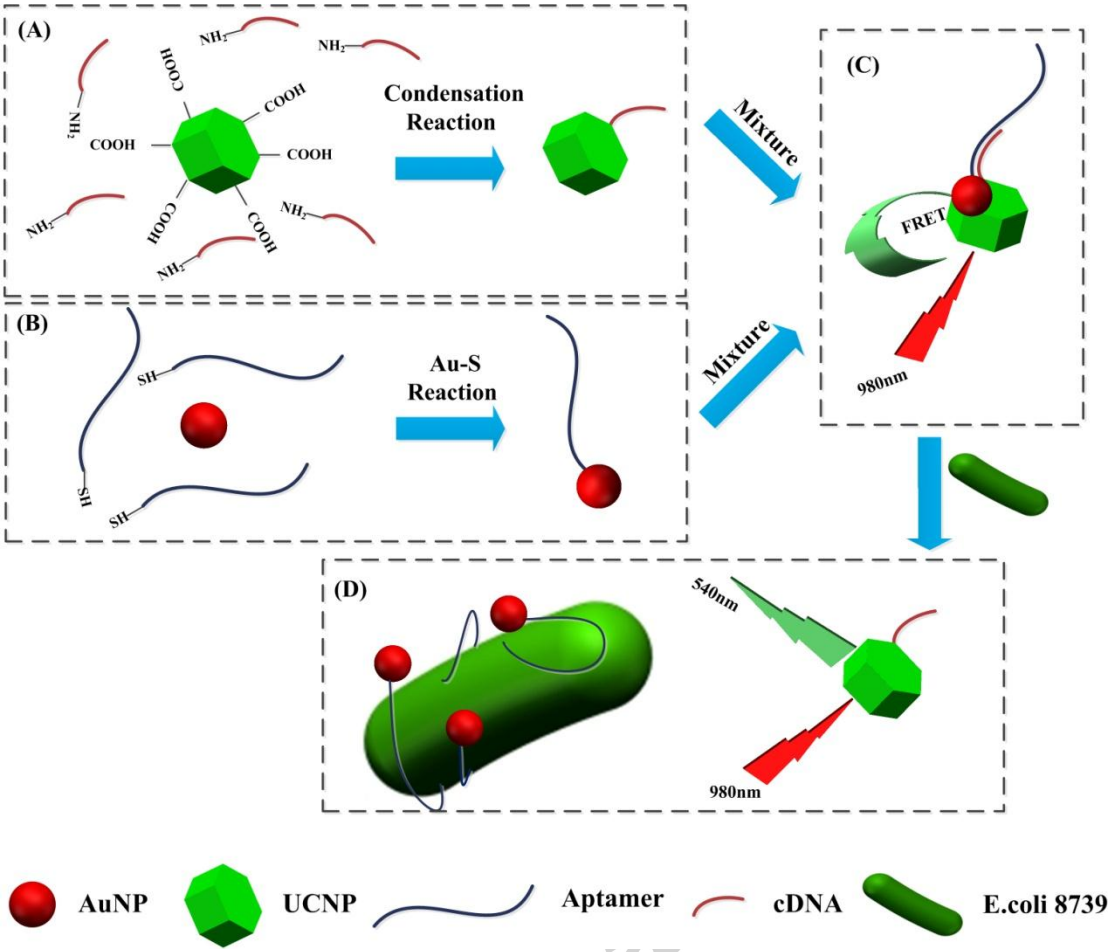

Figure 1. Schematic illustration of upconversion nanoparticles based FRET aptasensor for rapid and ultrasenstive bacteria detection. (A) The amino-modified complementary DNA of the aptamer is attached to the carboxyl-functionalized UCNPs by condensation reaction (B) Conjugating thiol-modified aptamers to the AuNPs through Au-S chemistry. (C) The FRET system is established between a donor-acceptor pair: UCNPs-cDNA hybridized with AuNPs-aptamers. (D) By introducing target bacteria into the FRET system, aptamers preferentially bind to target bacteria resulting in the dissociation of cDNA, thereby aptamers-DNA pairs are destroyed and the green fluorescence recovers.

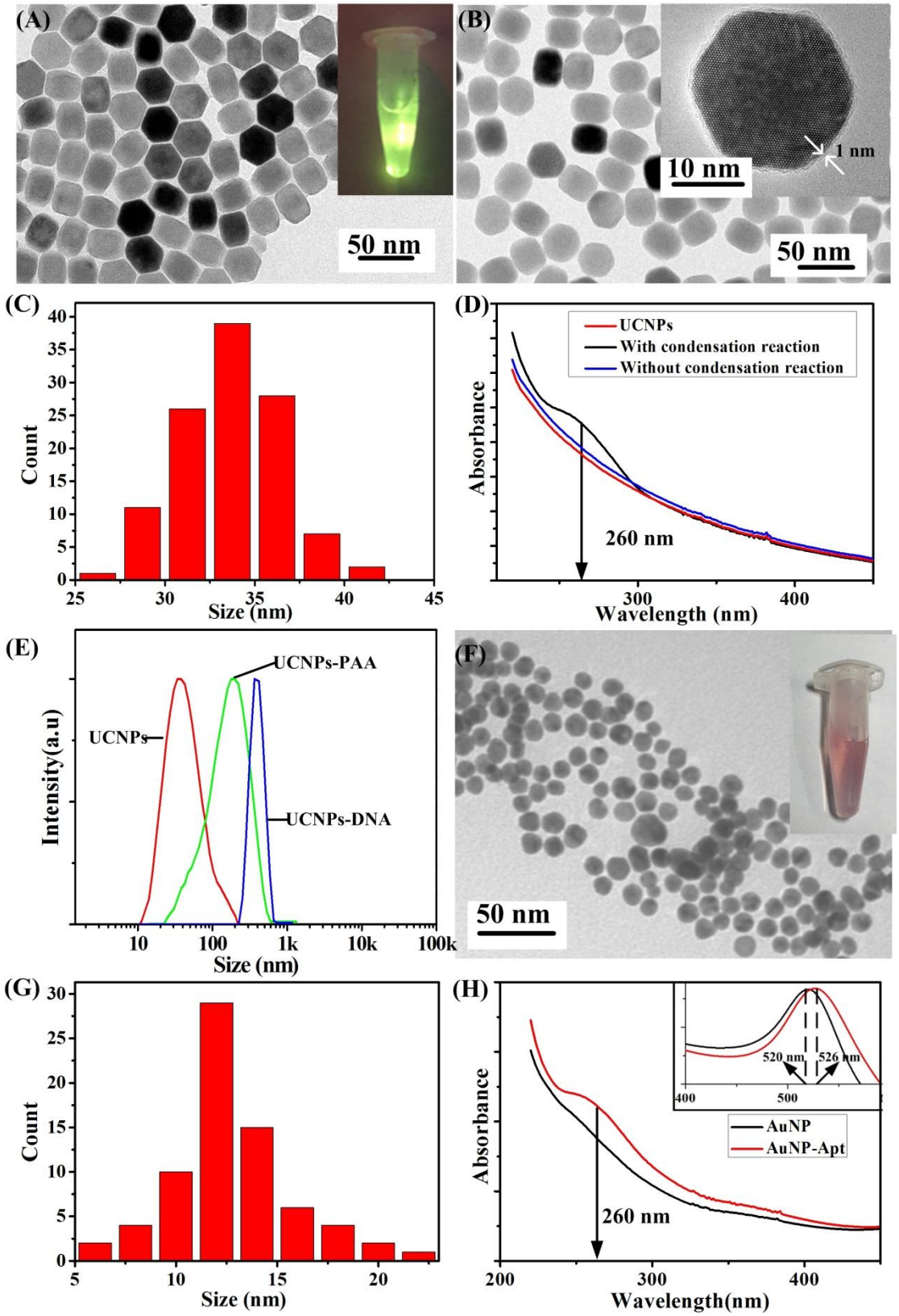

Figure 2. Characterization of UCNPs and AuNPs. (A) TEM of UCNPs, inset shows photograph of UCNPs excited by a 980 nm laser. (B) TEM of PAA modified UCNPs, inset shows the HRTEM image. (C) The size distribution of UCNPs. (D) The

UV-vis absorption spectra of DNA molecules and UCNPs complex. (E) DSL of UCNPs, UCNPs-PAA, UCNPs-PAA-cDNA. (F) TEM of AuNPs, inset shows photograph of AuNPs solution. (G) The size distribution of AuNPs. (H) UV-vis absorption spectra of AuNPs and AuNPs- aptamers. The inset shows the absorption peak of AuNPs sample experiences a slight red shift from 520 nm to 526 nm.

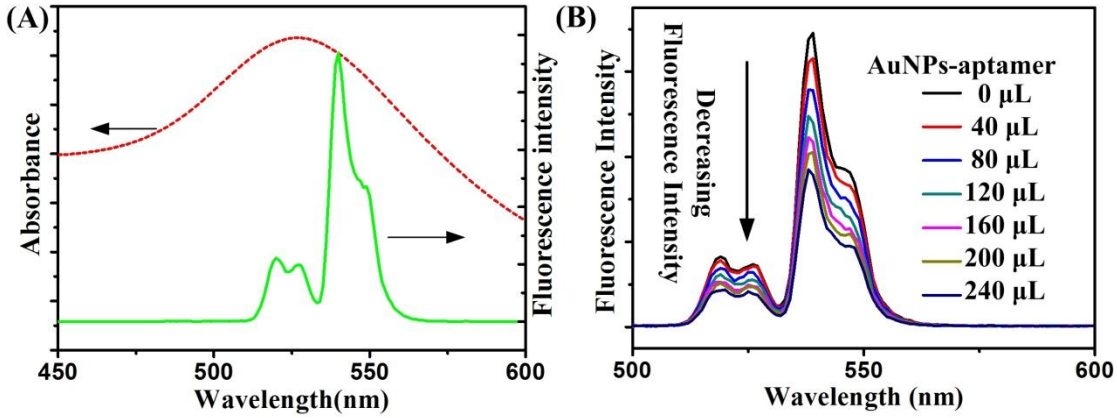

Figure 3. The spectral overlap of AuNPs and UCNPs. (A) UV-vis absorption spectrum of AuNPs (dashed line) and upconversion fluorescence emission spectrum of UCNPs (solid line). (B) The FRET between UCNPs-cDNA and AuNPs-aptamers. The molarity of UCNPs and AuNPs are 1 nM and 4.3 nM in the stock solution, respectively.

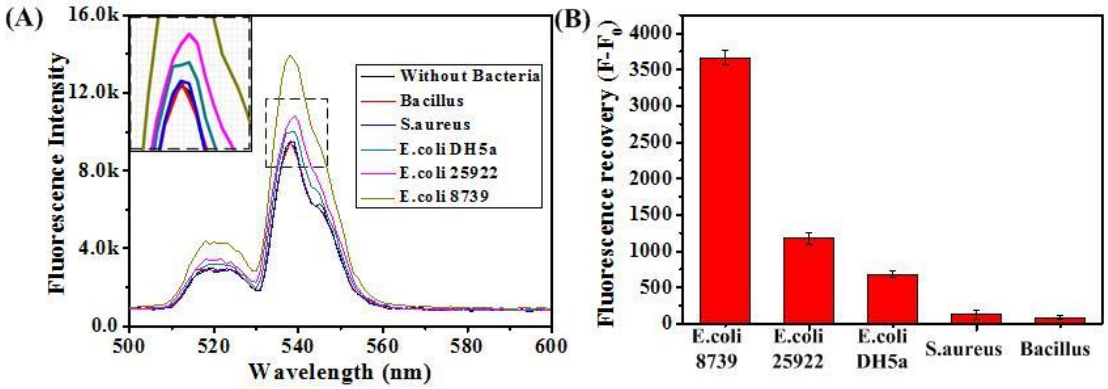

Figure 4. Change in upconversion fluorescence with varying types of bacteria. (Concentration of each bacteria was 10^4 cfu/mL.) (A) Fluorescence recovery results of different types of bacteria. (B) Quantification analysis of fluorescence recovery response for different types of bacteria.

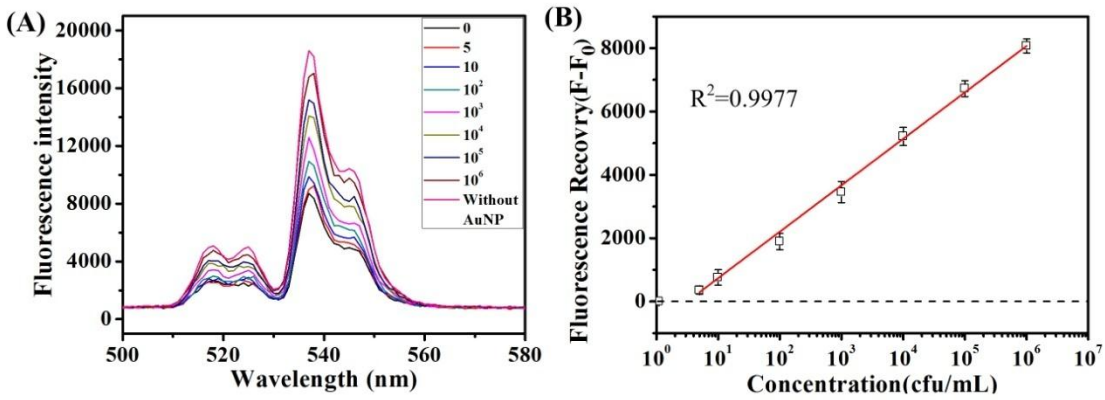

Figure 5. Detection of target bacteria with different concentrations. (A) Fluorescence recovery results of target bacteria with different concentrations. (B) Standard curve of relative upconversion fluorescence intensity ($F- F_0$) versus bacteria concentration.

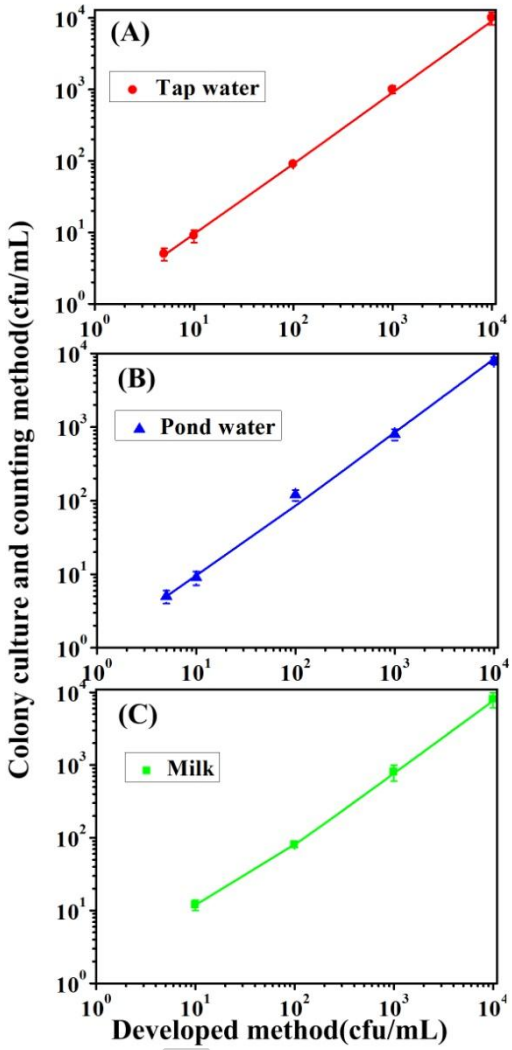

Figure 6. Relationship between the developed method and the official standard method for E.coli ATCC 8739 detection in (A) tap water, (B) pond water and (C) milk.

（此上两空行不能删除，是为 EndNote 的参考文献列表所预留